2025 IEEE Intelligent Vehicles Symposium (IV)
June 22-25, 2025. Cluj-Napoca, Romania

Influence of Autonomous Vehicle Interior Design on Occupant Injuries

Lukas Rozek[1], Andrew Harrison[2], Christian Birkner[1]

***Abstract*— In highly automated vehicles, the conventional roles of driver and passenger are transformed. This paradigm shift presents novel opportunities for the design of the vehicles interior. Recent research has demonstrated that occupants prefer to sit facing each other in highly automated vehicles, e.g., in living room configuration, in addition to conventional seating arrangements. However, studies have indicated that the restraint systems currently employed in new interior concepts do not achieve the desired effect. The shuttle, developed as part of the AWARE2ALL project funded by the European Union, was simulated in a sled test environment, undergoing various modifications to assess the necessary vehicle structures for ensuring occupant restraint. It was determined that reducing the forward movement of the occupant leads to a successful reduction in loads on the occupant. Incorporating a footrest within the design has emerged as a key element in reducing loads among occupants.**

***Index Terms*— highly automated vehicle, THOR-AV, passive safety, airbag, occupant injury.**

2025 IEEE Intelligent Vehicles Symposium (IV) | 979-8-3315-3803-3/25/$31.00 ©2025 IEEE | DOI: 10.1109/IV64158.2025.11097519

I. Introduction

Vehicles with SAE Level 4 or above autonomous driving systems [1], in which the occupants no longer act as driver, do not require conventional vehicle interior elements such as steering wheels or pedals. This change opens new possibilities for the design of the interior [2], [3]. The UNICARagil project, as referenced in [4], includes a user study that explores how interiors can be designed for autonomous vehicles. Research studies [5] and [6] describe various seating arrangements in highly automated vehicles, shown in Figure 1. The most common seat configurations include the conventional arrangement (forward-facing seats), the rotated arrangement (conversation position), and the ”living room” concept, which allows various combinations of interior design. In the forward-facing configuration, the first row of seats can feature a dashboard of the traditional vehicle interior design, similar to the rotated configuration. In contrast, occupants seated in the living room concept take on the role of passengers and the dashboard is omitted entirely. As indicated in [5], the seat positions can be rotated freely, and the backrests can be reclined, resulting in a novel spatial configuration. The seat positions diverge from the conventional arrangement. As indicated in [5], the restraint systems typically found in traditional vehicle designs are unable to safely restrain occupants and minimize injuries in the event of an accident unless new approaches are employed, e.g. current restraint systems are not designed for reclined seating positions. In [7], the feasibility of rotating seats was investigated. For conventional restraint systems to be employed effectively, the seat must be capable of unrestricted rotation around its vertical axis during periods of regular operation. However, in the event of an imminent crash, the seat is rotated into the driver’s position, thereby enabling the effective restraining of occupants by the traditional restraint systems [7]. Furthermore, the impact of the backrest and seat cushion inclination was examined in [8]. Luttenberger et al. [8] evaluated the efficacy of a ”safety vest” and a ”head containment system” in conjunction with the standard three-point seatbelt. These systems represent an extension of the conventional three-point seatbelt, developed to address the specific challenges posed by the evolving vehicle interior design.

In [9], the impact of varying seating positions in a conventional vehicle setting, is examined. Their findings demonstrate that even minor alterations in seating posture, such as crossing the legs, can have a considerable influence on the efficacy of restraint systems and the kinematics of occupants in the event of an accident. Yang et al. [10] investigated the seating positions in autonomous vehicles. The posture of the occupants is determined by the activity they perform while driving, e.g. eating or working, the so-called non-driving posture (NDP). The most frequently chosen seating position (forward seating occupant) is similar to the current driving postures in conventional vehicles [10].

While current research has focused on the impact of various body postures on occupant safety, the specific relationship between standard seating positions and the occurrence of injuries remains an important area. It is essential to gain insights into how the various elements of the vehicle interior affect injury outcomes in these conventional seating arrangements. Such understanding is crucial for the interior design of autonomous vehicles and occupant protection. This paper aims to analyze these relationships and identify the key factors contributing to injury risks in standard seating positions.

II. Methodology

This study aims to examine the impact of vehicle interior design on the functionality and performance of restraint systems, as well as the interaction between occupants and these systems. The vehicle interior from the AWARE2ALL project [11] is employed during the present investigation. The autonomous shuttle consists of four seats arranged in a face-to-face configuration (Figure 1C). The elemental configuration of the simulation model is based on the UMV People Mover, developed by ”Deutsches Zentrum für Luft-

[1]Technische Hochschule Ingolstadt, CARISSMA Institute of Safety in Future Mobility (C-ISAFE), Ingolstadt, Germany, e-mail: {lukas.rozek, christian.birkner}@thi.de

[2]Deutsches Zentrum für Luft- und Raumfahrt e.V. (DLR), Institut für Fahrzeugkonzepte, Stuttgart, Germany, e-mail: andrew.harrison@dlr.de

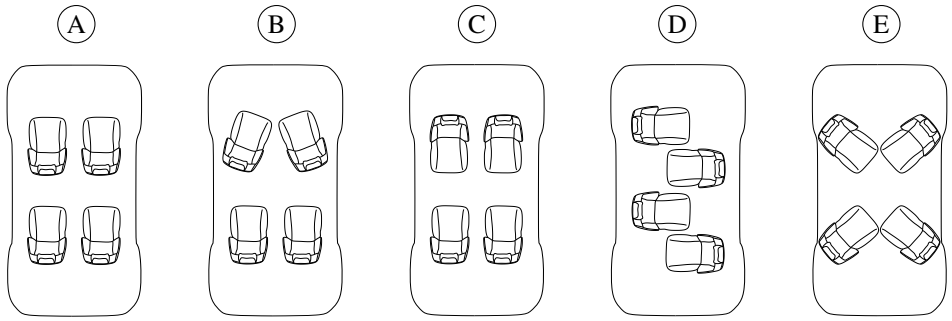

Fig. 1. Seating configuration in autonomous vehicle [forward-facing (A); rotated arragement (B), living room (C-E)], according to [5], [6].

und Raumfahrt e.V." (DLR) [12]. The integrated seats were derived from the open-source finite element (FE) model of the Toyota Camry from 2012 [13] and adapted to align with the necessities of the shuttle. The restraint systems, consisting of seatbelts and airbags, were developed as part of the AWARE2ALL project. The seat-integrated three-point seatbelt contains a pyrotechnic belt pretensioner on the shoulder belt. Furthermore, the belt parameters, such as material definition, have been derived from the open-source finite element model of the National Highway Traffic Safety Administration (NHTSA) Honda Accord from 2014 [14]. The airbag is L-shaped, contains a hybrid gas generator, and is attached to the vehicle ceiling, as in the EU project AWARE2ALL. A 50 kph full-frontal crash pulse provided by DLR with the sled test environment developed in AWARE2ALL, has been identified as particularly critical for occupant safety and was used in this study. The crash pulse exhibits an initial acceleration spike of 22 g, characteristic of early contact with limited energy-absorbing structures. This is followed by a brief attenuation and subsequent rise to a peak of 39.4 g as additional structural elements engage in energy absorption. The pulse exhibits a characteristic curve, and the acceleration and timing are within the operational parameters of safety restraint systems.

The finite element Anthropometric Test Dummys (FE-ATDs) are employed as occupant models. This study uses a forward-facing, 50-percentile male dummy (THOR-AV-50M) from Humanetics [15]. As can be seen from the literature review, posture and seating position are factors that influence the injury severity in a crash [9], [10]. The "in-position" occupant position is considered to classify the injuries in the subsequent studies according to consumer protection and legal requirements.

Eight load cases were defined for the study, as outlined in the following section. The initial situation in AWARE2ALL serves as baseline for adding components in each subsequent load case, continuing until the interior of today's vehicles is reached in Case 6. The methodology enables the assessment of the influence of individual components (cases 1–3) and subsequent combinations (cases 4–6 and 8) on occupant injuries. Based on these conclusions, recommendations for interior design can be derived. The load cases are as follows:

Baseline: In this configuration, the occupant is positioned following the specifications set in the AWARE2ALL project. The dummy is seated with their legs extended. The legs are positioned so that the feet are placed flat on the floor. The lower leg is positioned vertically to the floor, with an angle of 81° to the thigh, as demonstrated in Figure 2. A solid line illustrates the Baseline position.

Case 1: A footrest (Figure 2(*a*)) is introduced to the baseline situation. In this instance, the footrest replicates the angled floor panel typically observed in conventional vehicles on the passenger side. The angle between the upper and lower leg is now 110° and the feet are arranged on the angled footrest. The dummy positioning was performed according to the EuroNCAP Frontal full width (FW) protocol [16]. As in the Baseline position, it was adapted to the existing conditions in the shuttle, with the arms placed on the upper thighs, as there is no steering wheel.

Case 2: The Baseline is extended by adding an airbag (Figure 2(*b*)). As illustrated, the occupant's position is maintained in the baseline case. The airbag is fixed in position by a plate located behind it. This sheet metal is designed to simulate the fixation of the airbag in a conventional vehicle by a dashboard and windshield to ensure proper occupant restraint.

Case 3: A knee bolster (Figure 2(*c*)) is added to the Baseline. As in the previous cases, this extension is intended to imitate a dashboard. The knee bolster is positioned 167 mm away from the knee joint. The alignment has been taken from the dashboard of the Toyota Yaris FE model [17] and integrated into the simulation as a simplified sheet metal plate.

The objective of Cases 1 to 3 is to demonstrate the fundamental impact of the individual measures. The following cases combine earlier mentioned cases to confirm the effectiveness of the measures in question.

Case 4: Combination of Cases 1 and 3. The interior of the shuttle includes a footrest (*a*) and a knee bolster (*c*). The dummy is positioned according to the position in Case 1.

Case 5: Case 1 is combined with Case 2. The airbag (*b*) is extended with a footrest (*a*).

Case 6: Cases 1 to 3 have been merged. In this case, the vehicle's interior is configured according to the arrangement observed in existing vehicles. According to Figure 2 (*a*) + (*b*) + (*c*) have been added in this case.

A seat-integrated seatbelt is installed in all cases, including the Baseline, similar to the Shuttle from AWARE2ALL. In the remaining Cases 7 and 8, a seatbelt with alternative connections is used to confirm the impact of the previous investigations on the occupant in the event of a collision with other seatbelt connections. The Position of the D-ring is changed by (Δx = 0 mm, Δy = 116 mm, Δz = 130 mm), to imitate a position according to a D-ring attached to the B-pillar in a conventional vehicle. The anchor point is no longer attached to the seat frame but to the floor panel, as in conventional vehicles. The position of the buckle is analogous to that of the seat-integrated concept.

Case 7: The configuration is identical to that of the Baseline, with the exception of the non-integrated seatbelt (Figure 2(*d*)).

Case 8: This configuration combines Case 6 (Cases 1, 2 and 3) ((*a*) + (*b*) + (*c*)) with a non-integrated seatbelt from Case 7 (*d*), which corresponds to the situation in conventional vehicles.

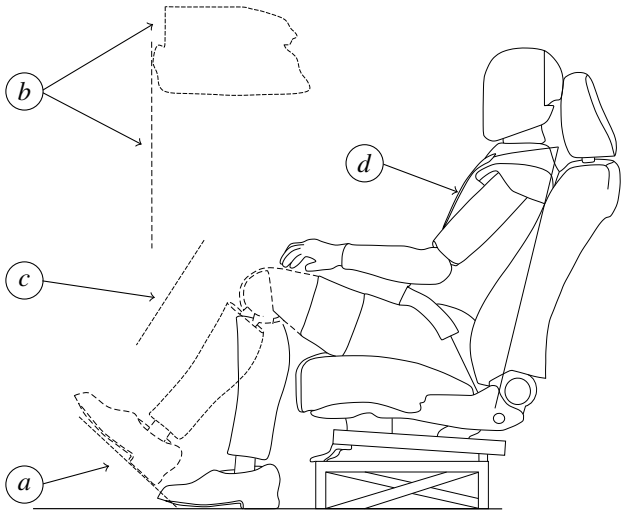

Fig. 2. Schematic of simulation setup (THOR-AV-50M (ATD)) with modifications indicated by dashed lines. The modifications consist of a footrest (*a*), an airbag with a plate to hold it in position (*b*), a knee bolster (*c*), and a seat-integrated or non-seat-integrated seatbelt (*d*). For simplicity, only the seat-integrated seatbelt is shown.

III. Results and Discussion

Table II presents the study's outcomes, comparing all modified versions (Case 1 to Case 8) with the baseline configuration. The percentage changes are documented in each respective cell. A negative cell value indicates an improvement or reduction in load has been achieved compared to the Baseline. The injury criteria for the respective body regions are derived from the load criteria for the THOR-50M [18], as the THOR-AV-50M utilized in the study does not currently have any published load criteria. Four body regions are considered, further subdivided into different measuring points. For the head, the Brain Injury Criteria (BrIC), the Head Injury Criterion (HIC_{15}), and the maximum head acceleration (a3ms) are evaluated.

The HIC_{15} can be calculated according to [18]:

$$HIC_{15} = \left| (t_2 - t_1) \left[\frac{1}{t_2 - t_1} \int_{t_1}^{t_2} a(t)\, dt \right]^{2.5} \right|_{\max}, \quad (1)$$

for $(t_2 - t_1) \leq 15$ ms.

For calculating the BrIC, the maximum angular head velocities in the x-, y- and z-axis and the critical angular velocities are used in the formula below by [18]:

$$BrIC = \sqrt{\left(\frac{\omega_x}{\omega_{xC}}\right)^2 + \left(\frac{\omega_y}{\omega_{yC}}\right)^2 + \left(\frac{\omega_z}{\omega_{zC}}\right)^2}, \quad (2)$$

with:

TABLE I
Critical maximum angular velocity [18]

Critical maximum angular velocity	Rad/s
ω_{xC}	66.25
ω_{yC}	56.45
ω_{zC}	42.87

The shear and tension forces and the neck extension are considered for the neck region.

The chest compression is calculated using four Infra-Red Telescoping Rods for the Assessment of Chest Compression (IR-TRACCs) [19]. The forces on the left and right acetabulum are evaluated for the pelvis region.

The knee displacement is also considered, primarily to assess the effects of different interior systems to the knee slider results with the inclusion of the knee bolster. Thereby providing insights to the effectiveness of the knee bolster in restraining the occupant and whether critical injury values were reached in the knee injury metric.

In summary, the results indicate that deployment of the airbag reduces head and neck injuries by 39 % on average, with less efficacy with introduction of more interior systems.

However, the results indicate the necessity for interior systems in addition to the seatbelt to prevent significant occupant excursions to reduce injury metrics in the torso, and pelvic regions. To facilitate a more in-depth discussion of this study, the corresponding results are shown in Table II as percentage changes of injury metrics with individual or multiple interior systems applied. The results are normalised against the Baseline and the boldened text signifies an increase to the injury metric.

An analysis of the simulation results indicates that including a footrest (*a*) reduces loads compared to the baseline scenario. A comparison of the simulations between the baseline scenario and Case 1 reveals that there is no load path for energy reduction via the legs in the Baseline. Therefore, the energy must be absorbed solely by the seatbelt. The occupant experiences significant motion in the direction of the crash (along the x-axis). In Case 1,

TABLE II

PERCENTAGE CHANGES OF INJURY DATA BETWEEN BASELINE AND MODIFICATIONS (< 0 = IMPROVEMENT TO BASELINE).

	Baseline	**Case 1** (*a*)	**Case 2** (*b*)	**Case 3** (*c*)	**Case 4** (*a*)+(*c*)	**Case 5** (*a*)+(*b*)	**Case 6** (*a*)+(*b*)+(*c*)	**Case 7** (*d*)	**Case 8** (*a*)+(*b*)+(*c*)+(*d*)
Head									
BrIC	0.00	-17.27	-32.53	-15.15	-17.27	-16.26	-19.90	-1.92	-9.60
HIC_{15}	0.00	-37.96	-40.11	-49.57	-38.26	-35.47	-33.30	-25.93	-21.94
a3ms	0.00	-41.37	-38.96	-44.53	-42.81	-40.24	-36.37	-24.54	-30.61
Neck									
Max. Shear force	0.00	-12.18	-51.20	-2.79	-5.79	-40.82	-43.81	-9.18	-25.35
Max. Tension force	0.00	**0.67**	-17.85	-0.37	-1.08	-12.48	-9.32	**11.56**	**0.87**
Max. Extension	0.00	-4.26	-53.01	-10.20	**2.26**	-41.11	-31.65	**16.58**	-13.55
Chest deflection									
upper left	0.00	-34.81	-1.91	-26.09	-41.53	-20.51	-21.52	-6.35	-6.30
upper right	0.00	-21.49	**10.20**	-15.67	-19.62	**0.89**	**4.98**	-1.57	**19.54**
lower left	0.00	-68.05	**6.71**	-29.68	-71.22	-48.44	-59.38	-5.04	-58.93
lower right	0.00	-31.98	**15.60**	-9.40	-37.59	-14.97	-28.49	**7.81**	-19.67
Pelvis									
Acetabulum force (left)	0.00	-33.46	-11.48	**17.54**	-27.15	-33.79	-23.56	**9.18**	-38.00
Acetabulum force (right)	0.00	-41.10	-1.84	-41.09	-45.92	-33.32	-48.15	**11.13**	-36.94
Knee displacement									
Knee slider left	0.00	-57.45	-9.34	**11.01**	-72.83	-67.27	-49.41	**14.51**	-48.57
Knee slider right	0.00	-59.9	**1.97**	**32.27**	-64.39	-77.36	-63.88	**12.62**	-65.76

the legs resting on the footrest create an additional load path for energy dissipation. The footrest also decreases the occupant's movement in the x-direction, reducing the load in the pelvic region by 34 % to 41 %.

The unequal reduction can be explained by the slight rotation of the occupant around the vertical z-axis. The support and the resulting reduction in movement along the x-axis reduces the amount of energy dissipated by the seatbelt, causing less rotation of the upper body forward around the y-axis and less compression of the chest. With less rotation of the upper body, the impact energy of the head on the thighs is reduced, resulting in lower head acceleration and associated head loads.

By adding an airbag (*b*) to the baseline shuttle (Case 2) as illustrated in Figure 2, loads in the head, neck and pelvis region are reduced, and an increased load on the thorax and ribcage can be noted ($\leq$ 16 %). The overall forward movement of the occupant will not be diminished solely by using an airbag. Consequently, in addition to the seatbelt, the airbag further compresses the thoracic area.

Up to 53 % of neck loads and 39 % of head loads have been reduced, partially due to preventing impact between the head and thighs. When deployed, the lower part of the L-shaped airbag is fully inflated by expanding gas. Because of that, the upward movement of the thighs is limited while permitting the upper body to rotate. After inflation, the airbag is clamped between the plate on the back of the airbag and the occupant's thoracic area. Along with the movement of the upper body, this configuration increases the compression of the ribcage. The design effectively reduces excessive forces on the neck. Additionally, the airbag surrounds the head, absorbing a significant amount of the energy generated by the upper body movement.

In Case 3, the knee bolster (*c*) is crucial in significantly restraining the occupant's forward movement. The contact between the knee and the knee bolster creates a load path for energy dissipation. Compared to the baseline scenario, the rotation of the upper body is reduced, and there is a rebound effect after reaching the knee bolster. This rebound minimizes the impact energy of the head on the thighs, consequently decreasing the loads on the head (15 - 50 %) and neck ($\leq$ 10 %). The reduced forward translation also results in lower loads in the chest region (10 - 30 %). However, it is important to note that there are significant displacements at the knee sliders (11 - 32 %) due to contact with the knee bolster.

The combination of the footrest (*a*) and knee bolster (*c*) in Case 4 reduces loads in all body regions. Similar to Case 1 (footrest), an additional load path for dissipating energy through the legs into the vehicle structure is present. The knee bolster (*c*), in turn, adds another load path to the shuttle. Accordingly, two additional load paths have been added to the shuttle besides the seatbelt. Supporting the legs reduces the forward movement of the lower body. The contact between the knee and knee bolster occurs in a diminished manner. The rotation of the upper body is further reduced, resulting in decreased energy upon contact of the head with the thighs and, thus, a reduction in loads compared to the Baseline. It is notable that, in comparison to Case 3 (knee bolster (*c*)), the knee displacements and, consequently, the impact load on the knee bolster can be mitigated by a combination of two measures in addition to

the chest and pelvis loads.

An explicit comparison of Cases 1 and 3 and their combination (Case 4) reveals the effectiveness of the modifications. The three cases show similar head loads. Regarding these, either a footrest or a knee bolster can be used, as only minor improvements can be seen with their combination. The analysis of the chest indentation shows that a combination of both measures in Case 4 solely achieves a 7 % improvement, when a knee bolster is added to Case 1.

As already discussed in the previous cases, Case 3 shows high loads in the pelvic area. In combination, these lead to a reduction in the effectiveness of the footrest and an increase in the uneven load on the pelvis. For instance, the disparity in the load on the left and right acetabulum is 8 % in Case 1 and 19 % in Case 4.

In Case 5, the combination of the footrest (*a*) and airbag (*b*) reduces the load on the head and neck, as already seen in Case 2. This decrease is primarily due to the use of the airbag. It is worth noting that the loads in the thoracic region have decreased, compared to the Baseline, but especially in direct comparison to Case 2 (airbag (*b*)). The explanation can be found in Case 1. By supporting the legs on the footrest, energy is dissipated through this load path, reducing the forward movement of the occupant, which is reflected in the reduction of chest loads.

In Case 6 (combination of footrest (*a*), airbag (*b*), and knee bolster (*c*)), a reduction in loads in all body regions is visible compared to the baseline scenario. However, in comparison to Case 5 (footrest (*a*) and airbag (*b*)), the inclusion of the knee bolster (*c*) only decreases the overall chest compression by 0.35 %, exhibiting an average 11.5 % increase to upper chest loading and 12.2 % decrease in the lower chest region. Furthermore, evaluating the head region, the inclusion of the knee bolster exhibited a 3 % increase to acceleration-based injury metrics, whereas the rotational velocity injury metric (BriC) reduced by 3.6 %. This suggests that the knee bolster has a greater effectiveness in reducing the upper torso rotation, also implied by the reduction (3 %) in the neck shear force. Although less rotation is exhibited, a greater linear acceleration is evident in the head and neck region, thus increasing the neck tension and extension forces (3.2 % and 9.4 % respectively). As previously mentioned, the influence of the airbag dominates the risk of injuries in the head and neck regions. Therefore, it stands to reason that the airbag could be fine-tuned to lessen the effects of the knee bolster presence, however the performance would be very sensitive to different size or position of the occupant. It is also worth noting that the presence of the knee bolster in each case with a seat mounted seatbelt increases the load disparity between the acetabulum's left and right side in comparison to cases without (*c*). This indicates that the pathing required on the seat-mounted seatbelt sufficiently holds tightly across the lap-belt upon knee bolster impact, reducing the contact force of the knee bolster and force transferred to the acetabulum. Whereas the anchorage location (left side of occupant) has greater freedom to move and therefore impacts the knee bolster with greater force which is transferred directly to the left side of the acetabulum. It is worth noting that inclusion in Case 8 that the greatest performance is witnessed for pelvic loading, with similar load distribution between the acetabulum sides. This could be due to the B-pillar location (D-ring), that when the belt passes through the buckle slipring, a more distributed pre-tensioning force is applied across the length of the lap belt.

In Case 7, which examines the use of a non-seat-integrated seatbelt (*d*), the focus is on assessing the impact of the seatbelt as an independent component in vehicle design on load distribution. As anticipated, this modification results in a reduction in chest loading in the upper thorax region. This reduction can be attributed to the higher attachment point of the D-ring and the associated belt path. The lower part is getting compressed more strongly than in the baseline scenario. The explanation can be found in the narrowly different belt pathing.

With the D-ring positioned higher, the seatbelt is redirected at the shoulder, varying from the baseline configuration. Thus, the upper body rotates more, which increases the bending of the spine and neck. While this adjustment leads to a decrease in rib loads and head acceleration, it also elevates the extension experienced by the neck. Additionally, when combined with forward movement, this configuration results in increased loads on the pelvis.

In the combination of the footrest (*a*), airbag (*b*), knee bolster (*c*), and non-seat-integrated seatbelt (*d*) in Case 8, there is a noticeable reduction in all body regions compared to the baseline scenario. In a similar fashion to Case 6, the footrest (*a*), airbag (*b*) and knee bolster (*c*) provide the main pathways for energy dissipation and mitigation of occupant excursion. Overall the lower regions display similar improvements to the baseline, in which Case 8 exhibits an average 1 % improvement to Case 6 in combined pelvic and knee displacement metrics. However, further comparing cases 8 to 6 highlights that the conventional belt location (D-ring on B-pillar) does not provide optimal effectiveness in torso and neck regions. This is shown through increased head risk of injury (9 %), neck (15.5 %) and average chest compression (4.8 %).

IV. Conclusion

In conclusion, reducing the occupant movement is essential to effectively distributing loads. As expected, introducing components to reduce the occupant excursion through the knee bolster or footrest successfully reduced the forward excursion of the occupant whilst the airbag significantly reduced the risk of neck and head injuries. The study evaluated the effectiveness of various interior systems as stand-alone and combined to permit alternative vehicle interior concepts with the emergence of new interior configurations enabled by autonomous driving technology. To this end, the study demonstrated that not enacting any interior configuration alone is sufficient to support the enhancement of all injury regions, often resulting in a trade-off between improving

one region and another. Furthermore, it is evidenced that including all interior systems leads to a degradation in the improvements witnessed. This suggests that not all systems are necessary and cannot be identified for specific regions or behaviors evidenced by the individual vehicle. Overall, the most efficient systems to implement were in Case 5. The inclusion of the airbag provided mitigation to the injuries of the neck and head regions whilst the footrest sufficiently lessened occupant excursion and managed the kinematics for effective deployment of belt and airbag systems.

Furthermore, the study provides explanations and insights into the kinematic response of occupants with varying interior components that could be used as a guide for defined interior configurations and facilitating further research and development of vehicle interiors to enable the development of highly automated vehicles. It is important to note that Case 8 utilized the D-ring in the B-pillar location, which may not be feasible in a living room concept or a shuttle design.

V. Limitations and Future Work

Since only load limit values exist for the THOR dummy currently, the loads and their changes compared to the baseline configuration in this study can only be presented as percentage changes, and the classification of the type of injury and its significance for the occupant cannot be determined. Furthermore, the results obtained are within the verifiable limits of the FE model.

An expansion of the study to include the THOR-AV-5F (five percentile female dummy) is planned in future investigations. Furthermore, the collected results will be examined using Human Body Models (HBMs), and the correlation of injury criteria between established dummys (ATDs) and HBMs will be validated.

Acknowledgement

This work has received funding from the European Union's Horizon Europe research and innovation programme under grant agreement number 101076868, project AWARE2ALL.

References

[1] SAE International, "Taxonomy and Definitions for Terms Related to Driving Automation Systems for On-Road Motor Vehicles," SAE International, Standard SAE J3016, 2021.

[2] Yang, Yucheng and Fleischer, Martin and Bengler, Klaus, "Chicken or Egg Problem? New Challenges and Proposals of Digital Human Modeling and Interior Development of Automated Vehicles," in *Advances in Additive Manufacturing, Modeling Systems and 3D Prototyping*. Cham: Springer International Publishing, 2020, pp. 453–463.

[3] A. Filatov, J. M. Scanlon, A. Bruno, S. S. K. Danthurthi, and J. Fisher, "Effects of Innovation in Automated Vehicles on Occupant Compartment Designs, Evaluation, and Safety: A Review of Public Marketing, Literature, and Standards," SAE International, Tech. Rep. 2019-01-1223, 2019, WCX SAE World Congress Experience.

[4] A.-L. Köhler *et al.*, "How Will We Travel Autonomously? User Needs for Interior Concepts and Requirements Towards Occupant Safety," in *28th Aachen Colloquium Automobile and Engine Technology*, 2019, pp. 809–836.

[5] S. Jorlöv, K. Bohman, and A. Larsson, "Seating Positions and Activities in Highly Automated Cars—A Qualitative Study of Future Automated Driving Scenarios," in *Proceedings of the International Research Council on Biomechanics of Injury (IRCOBI) Conference*, 2017, pp. 13–22.

[6] L. Hyncik, A. Talimian, J. Vychytil, J. Kleindienst, S. Gharbi, and P. Ziazopoulos, "Injury Assessment in Non-Standard Seating Configurations in Highly Automated Vehicles Using Digital Twin and Active Learning," *SAE Technical Paper*, 2023.

[7] J. Becker *et al.*, "Occupant Safety in Highly Automated Vehicles—Challenges of Rotating Seats in Future Crash Scenarios," in *Proceedings of the International Research Council on Biomechanics of Injury (IRCOBI) Conference*, 2020, pp. 381–397.

[8] P. Luttenberger *et al.*, "Assessment of future occupant restraint principles in autonomous vehicles," in *Proceedings of the International Research Council on Biomechanics of Injury (IRCOBI) Conference*, 2020, pp. 431–455.

[9] A. Leledakis, J. Östh, J. Davidsson, and L. Jakobsson, "The influence of car passengers' sitting postures in intersection crashes," *Accident Analysis & Prevention*, vol. 157, p. 106170, 2021.

[10] Y. Yang, J. N. Klinkner, and K. Bengler, "How Will the Driver Sit in an Automated Vehicle? – The Qualitative and Quantitative Descriptions of Non-Driving Postures (NDPs) When Non-Driving-Related-Tasks (NDRTs) Are Conducted," in *Advances in Intelligent Systems and Computing: Proceedings of the 20th Congress of the International Ergonomics Association (IEA) 2018*, S. Bagnara, R. Tartaglia, S. Albolino, T. Alexander, and Y. Fujita, Eds. Florence, Italy: Springer, Cham, 2019.

[11] AWARE2ALL Project, "AWARE2ALL - Awareness and Inclusive Accessibility for All," 2024, Accessed: 2024-10-24. [Online]. Available: https://aware2all.eu/

[12] M. Münster, G. Kopp, H. E. Friedrich, and T. Siefkes, "Autonomes Fahrzeugkonzept für den urbanen Verkehr der Zukunft," *ATZ-Automobiltechnische Zeitschrift*, vol. 122, no. 3, pp. 26–31, 2020.

[13] D. Marzougui, D. Brown, H. Park, C. Kan, and K. Opiela, "Development & Validation of a Finite Element Model for a Mid-Sized Passenger Sedan," in *Proceedings of the 13th International LS-DYNA Users Conference*, 2014.

[14] H. Singh, V. Ganesan, J. Davies, M. Paramasuwom, and Gradischnig, "Vehicle Interior and Restraints Modeling Development of Full Vehicle Finite Element Model Including Vehicle Interior and Occupant Restraints Systems For Occupant Safety Analysis Using THOR Dummies," National Highway Traffic Safety Administration, Washington, DC, Technical Report DOT HS 812 545, 2018.

[15] Humanetics Group, "THOR-AV 50M: Anthropomorphic Test Device for Autonomous Vehicles," accessed: 2025-01-16. [Online]. Available: https://www.humaneticsgroup.com/products/anthropomorphic-test-devices/autonomous-vehicle-atds/thor-av-50m/thor-av-50m

[16] Euro NCAP, *Frontal Full Width (FW) Test Protocol*, 2021, accessed: 2025-01-16. [Online]. Available: https://cdn.euroncap.com/media/67284/euro-ncap-frontal-fw-test-protocol-v121.pdf

[17] Center for Collision Safety and Analysis, "2010 Toyota Yaris Finite Element Model Validation Detail Mesh," accessed: 2025-01-10. [Online]. Available: https://doi.org/10.13021/G8CC7G

[18] M. Craig, D. Parent, E. Lee, R. Rudd, E. Takhounts, and V. Hasija. (2020) Injury Criteria for the THOR 50th Male ATD. Accessed: 2024-10-16. [Online]. Available: https://lindseyresearch.com/wp-content/uploads/2021/10/NHTSA-2020-0032-0005-Injury-Criteria-for-the-THOR-50th-Male-ATD.pdf

[19] Z. Wang and B. Watson, "An Algorithm to Calculate Chest Deflection from 3D IR-TRACC," *SAE Technical Paper*, 2016.